

NRC Publications Archive Archives des publications du CNRC

Attosecond photoionization of coherently coupled electronic states

Yudin, G. L.; Chelkowski, S.; Itatani, J.; Bandrauk, A. D.; Corkum, P. B.

This publication could be one of several versions: author's original, accepted manuscript or the publisher's version. / La version de cette publication peut être l'une des suivantes : la version prépublication de l'auteur, la version acceptée du manuscrit ou la version de l'éditeur.

For the publisher's version, please access the DOI link below. / Pour consulter la version de l'éditeur, utilisez le lien DOI ci-dessous.

Publisher's version / Version de l'éditeur:

<https://doi.org/10.1103/PhysRevA.72.051401>

Physical Review. A, Atomic, Molecular, and Optical Physics, 72, 5, 2005

NRC Publications Archive Record / Notice des Archives des publications du CNRC :

<https://nrc-publications.canada.ca/eng/view/object/?id=69ced6cd-cd17-4645-b6c1-9d2cd1b88dfa>

<https://publications-cnrc.canada.ca/fra/voir/objet/?id=69ced6cd-cd17-4645-b6c1-9d2cd1b88dfa>

Access and use of this website and the material on it are subject to the Terms and Conditions set forth at

<https://nrc-publications.canada.ca/eng/copyright>

READ THESE TERMS AND CONDITIONS CAREFULLY BEFORE USING THIS WEBSITE.

L'accès à ce site Web et l'utilisation de son contenu sont assujettis aux conditions présentées dans le site

<https://publications-cnrc.canada.ca/fra/droits>

LISEZ CES CONDITIONS ATTENTIVEMENT AVANT D'UTILISER CE SITE WEB.

Questions? Contact the NRC Publications Archive team at

PublicationsArchive-ArchivesPublications@nrc-cnrc.gc.ca. If you wish to email the authors directly, please see the first page of the publication for their contact information.

Vous avez des questions? Nous pouvons vous aider. Pour communiquer directement avec un auteur, consultez la première page de la revue dans laquelle son article a été publié afin de trouver ses coordonnées. Si vous n'arrivez pas à les repérer, communiquez avec nous à PublicationsArchive-ArchivesPublications@nrc-cnrc.gc.ca.

Attosecond photoionization of coherently coupled electronic states

G. L. Yudin,^{1,2} S. Chelkowski,¹ J. Itatani,^{2,*} A. D. Bandrauk,¹ and P. B. Corkum²

¹*Laboratoire de Chimie Théorique, Université de Sherbrooke, Sherbrooke, Québec, Canada J1K 2R1*

²*National Research Council of Canada, Ottawa, Ontario, Canada K1A 0R6*

(Received 15 March 2005; published 1 November 2005)

We study analytically the photoionization of a coherent superposition of atomic and molecular electronic states by an ultrashort, attosecond x-ray pulse. We show that the broad photoelectron spectrum contains detailed information about the time-dependent electron wave packet. The asymmetry of the photoelectron momentum distribution measures the momentum asymmetry of the initial bound-state wave packet. We show that molecular interference modulates the time-dependent photoelectron spectrum and asymmetry. The modulation also depends on the internuclear separation. The photoelectron spectrum and its asymmetry monitors coherent electron motion and in principle electron transfer on the attosecond time scale.

DOI: [10.1103/PhysRevA.72.051401](https://doi.org/10.1103/PhysRevA.72.051401)

PACS number(s): 33.80.Wz, 42.50.Hz

Photoionization is a classic tool for investigating atomic and molecular electronic structure. Recent advances in ultrashort laser-pulse technology enables experimentalists to synthesize and characterize ultrashort pulses in the attosecond time regime [1–5]. We show how these attosecond pulses can be used to measure attosecond bound-state electron dynamics.

Our method is based on broad bandwidth photoionization. Single-photon ionization from a stationary state produces photoelectrons that contain information on the optical pulse and the phase and structure (through the transition moment) of the initial state. If the state is known, measurement of the photoelectron spectra produced in the presence of a phased infrared field fully characterizes the attosecond pulse (see references in review [4] and more recent papers [6–8]); if, on the other hand, the attosecond pulse is known, measurement of photoelectron spectra produced from two or more coherently excited states determines all information on the associated bound-state wave packet.

We show that dynamic information is retained in the integrated momentum asymmetry of the photoelectrons. Specifically, if the molecule is aligned, wave-packet dynamics is revealed in the average photoelectron momentum along only one axis even with a broad angular window. This means that attosecond electron wave packets are observable in pump-probe experiments in which only a relatively small number of photoelectrons are needed for each delay.

Photoionization asymmetry [9,10] has already been used to measure the carrier envelope phase of intense few-cycle laser pulses [11]. Photoionization is also related to a proposal to measure bound-state electron dynamics during the attosecond generation process itself [12]. Attosecond single-photon ionization has three advantages over strong-field techniques. Specifically, we can: (i) measure a bound electron state that is not perturbed by a strong laser field, (ii) correlate photoelectrons to ion fragments so that we can specify the molecular internal states and alignment direction, and (iii) precisely

take into account the Coulomb potential in the molecular continuum.

We adapt a scheme used to study attosecond localization of an electron in a diatomic molecule [13] and to prepare a coherent superposition of molecular bound states. We show that asymmetric ionization can measure attosecond electron bound-state dynamics.

As theoretically tractable example that capture the essence of our approach, we consider the hydrogen atom with a coherent superposition of $1s$ (atomic state $|1\rangle$) and $2p_0$ (atomic state $|2\rangle$) bound states, and a H_2^+ molecular ion with a coherent superposition of two electronic states, $\sigma_g 1s$ (molecular state $|1\rangle$) and $\sigma_u 2p_0$ (molecular state $|2\rangle$). We assume that the H_2^+ molecular ion is aligned. Alignment can be effectively achieved experimentally for unstable molecules since, following ionization, the molecular fragments determine the alignment with high accuracy [14–16]. In our three-dimensional model, the molecular ion and electric field of the attosecond pulse are aligned along the z axis in Cartesian space.

We use a pump pulse with a slowly varying envelope and the resonant frequency $\Delta I_p = I_p^{(1)} - I_p^{(2)}$, where $I_p^{(1,2)}$ are the ionization potentials of the states $|1\rangle$ and $|2\rangle$ (unless stated otherwise, we use atomic units $e = m_e = \hbar = 1$). The pulse prepares a coherent superposition of two bound states,

$$\Psi_i(\mathbf{r}, t) = \alpha_1 \Psi_1(\mathbf{r}, t) + \alpha_2 \exp(i\phi) \Psi_2(\mathbf{r}, t), \quad (1)$$

where $\alpha_{1,2}^2$ are their populations ($\alpha_1^2 + \alpha_2^2 = 1$) and ϕ is an adjustable phase that depends on the excitation scheme. In the general molecular case, the excitation by the pump pulse generates a nuclear wave-packet on the repulsive state potential. The electron wave-packet time scale is given by the level separation (~ 300 asec). The relative nuclear motion is given by the relative slopes of the curves involved (~ 100 fs). These time scales remain well separated so the nuclei are considered fixed.

Each bound state of the H_2^+ ion is a molecular orbital that we approximate as a linear combination of atomic orbitals $\psi_{at}(\mathbf{r})$,

*Present address: Japan Science and Technology Agency 1-1 Oho, Tsukuba, Ibaraki 305-0801, Japan.

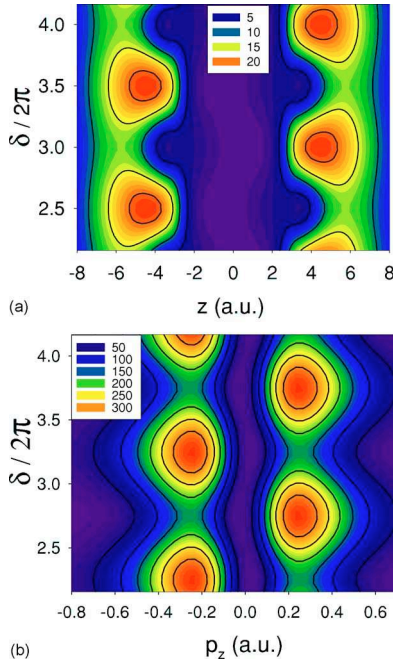


FIG. 1. (Color online) The molecular electron density in H_2^+ at the internuclear separation $R=6$ a.u. as a function of phase shift δ and coordinate z along the molecular axis in (a) coordinate representation and (b) its analog in momentum representation.

$$\Psi_{1,2}(\mathbf{r}, t) = N_{1,2} [\psi_{at}^{(1,2)}(\mathbf{r}_1) + \psi_{at}^{(1,2)}(\mathbf{r}_2)] \exp[iI_p^{(1,2)} t]. \quad (2)$$

The vectors $\mathbf{r}_{1,2} = \mathbf{r} \pm \mathbf{R}/2$, where \mathbf{R} is directed from the nucleus 1 to the nucleus 2. In our case, $\psi_{at}^{(1)}(\mathbf{r})$ and $\psi_{at}^{(2)}(\mathbf{r})$ are the hydrogenlike $1s$ and $2p_0$ wave functions with the variational Slater parameters a_1 and a_2 (see below) which are different functions of the R .

Figure 1(a) shows the coherent molecular electron density integrated over the cylindrical coordinate ρ as a function of the coordinate z and time-dependent phase shift $\delta(t) = \Delta I_p t - \phi$. $\delta(t)$ parametrizes the electron motion via the difference in ionization potentials ΔI_p , which depends on R . The corresponding electron density in the longitudinal momentum p_z is shown in Fig. 1(b). The position and momentum densities are 90° out of phase because the momentum is the derivative of the wave function. The internuclear separation in Fig. 1 is $R=6$ a.u. and the populations of the ground and excited states are $\alpha_1^2=0.1$ and $\alpha_2^2=0.9$. One can observe the electron “hop” from one nucleus to another with a period of $T = 2\pi/\Delta I_p$.

Now we consider single-photon photoionization induced by a probe attosecond x-ray pulse with vector potential $\mathbf{A}_x(t) = \mathbf{e}(A_0/2) \exp[-i\Omega_x t - (t-t_0)^2/2\tau^2]$, where Ω_x is the central frequency of the attosecond pulse and \mathbf{e} , A_0 , and t_0 are the linear polarization vector, amplitude, and peak of the pulse, respectively. We calculate the photoionization amplitude using the final two-center Coulomb wave function introduced in [17]. For photoelectron momenta $p \gg 1$ and $|pR \pm \mathbf{p} \cdot \mathbf{R}| \gg 1$, the direct molecular ionization transition amplitudes are determined by atomic amplitudes, $M_{mol}^{(1,2)} = N_{1,2} \chi M_{at}^{(1,2)}$, where the molecular interference factor

$$\chi = N_p [\exp(i\mathbf{p} \cdot \mathbf{R}/2) \Phi(-\mathbf{R}) + \exp(-i\mathbf{p} \cdot \mathbf{R}/2) \Phi(\mathbf{R})]. \quad (3)$$

$N_p = \exp(\pi/2p) \Gamma(1+i/p)$ is the normalization factor and $\Phi(\mathbf{R})$ is the hypergeometric function, $\Phi(\mathbf{R}) = F(i/p; 1; i(pR + \mathbf{p} \cdot \mathbf{R}))$. In the plane-wave approximation the factor χ becomes $\chi_{pw} = 2 \cos(\mathbf{p} \cdot \mathbf{R}/2)$.

The atomic and molecular attosecond photoionization amplitudes for the coherently coupled state (1) are given by

$$M_{coh} = M_0 [\gamma_1 M^{(1)} + \gamma_2 \exp[-i\delta(t_0)] M^{(2)}], \quad (4)$$

where $\gamma_k = \alpha_k \exp(-\omega_k^2 \tau^2/2)$, $\omega_k = p^2/2 + I_p^{(k)} - \Omega_x$, $k=1, 2$, and $M_0 = A_0 \tau (\pi/2)^{1/2} \exp(i\omega_1 t_0)$. The triple differential momentum spectrum is

$$d^3 P_{coh}(p, \theta, \varphi) = |M_{coh}|^2 p^2 dp d\Omega_e, \quad (5)$$

where $d\Omega_e = \sin \theta d\theta d\varphi$ is the solid angle.

Equation (5) describes the angle-resolved photoelectron spectrum. For a known attosecond pulse it contains all spatial and temporal information about the wave packet. However, retrieving this information would be difficult with current attosecond sources. To make attosecond wave-packet measurements experimentally feasible we introduce an asymmetry parameter

$$\Delta(p, \theta, \varphi) = \frac{d^3 P(p, \theta, \varphi)}{dp d\Omega_e} - \frac{d^3 P(p, \pi - \theta, \varphi)}{dp d\Omega_e}. \quad (6)$$

Integrating the differential probability (5) over momenta at θ and φ determines the integrated probability $P(\theta, \varphi)$. This defines the normalized integrated asymmetry

$$A(\theta, \varphi) = A^{(-)}(\theta, \varphi) / A^{(+)}(\theta, \varphi), \quad (7)$$

where $A^{(\pm)}(\theta, \varphi) = P(\theta, \varphi) \pm P(\pi - \theta, \varphi)$. The asymmetries (6) and (7) are independent of the azimuthal angle φ since the molecule is aligned along the z axis.

The dipole atomic photoionization amplitudes M_{1s} and M_{2p_0} are given by

$$M_{1s} = 2\sqrt{2} a_1^{3/2} N_p G_1(\mathbf{e} \cdot \mathbf{p})(p-i)(\pi p D_1^2)^{-1}, \quad (8)$$

$$M_{2p_0} = -4i a_2^{1/2} N_p G_2[(\mathbf{e} \cdot \mathbf{p})^2 8a_2^2(p-i)(2p-i) + p D_2(i-2pa_2) - ip(1+2ipa_2^2)](\pi p^2 D_2^3)^{-1}, \quad (9)$$

where the functions $G_k = \exp[-(2/p) \text{acot}(1/kpa_k)]$ and $D_k = 1 + (kpa_k)^2$, $k=1, 2$. From Eq. (4) we obtain

$$\Delta_{at}(p, \theta) = 2\pi A_0^2 \alpha_1 \alpha_2 \mu p^2 \text{Re}\{e^{-i\delta(t_0)} M_{1s}^* M_{2p_0}\}, \quad (10)$$

$$\Delta_{mol}(p, \theta) = N_1 N_2 |\chi|^2 \Delta_{at}(p, \theta). \quad (11)$$

The pulse-duration dependence of the asymmetry $\Delta(p, \theta)$ is described by the factor $\mu = \tau^2 \exp[-(\omega_1^2 + \omega_2^2) \tau^2/2]$. In the molecular case such a functional depends on R via $\omega_{1,2}$ and therefore exhibits maxima for certain τ at specific R . We further note that the asymmetry of the photoionization is directly proportional to the product $\alpha_1 \alpha_2$, i.e., the square root of populations. Therefore, it is relatively insensitive to the populations α_1^2 and α_2^2 . The asymmetries (10) and (11) de-

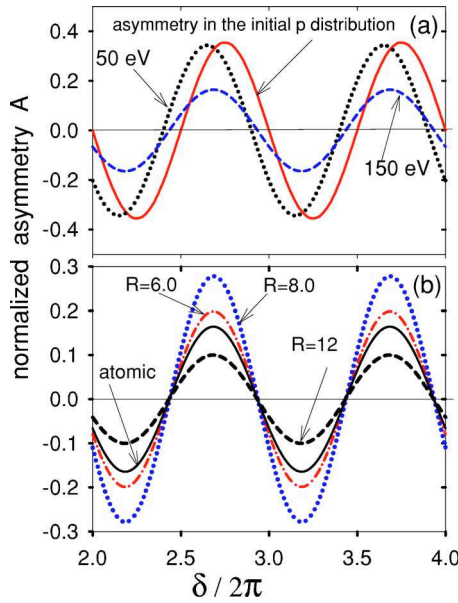


FIG. 2. (Color online) The asymmetries in (a) H atom and (b) H_2^+ molecule (for $R=6, 8,$ and 12 a.u.) as functions of the phase shift δ . The pulse duration is $\tau_{FWHM}=100$ asec. The photon energy and polar angle in Fig. 2(b) are $\Omega_x=150$ eV and $\theta=30^\circ$.

pend on the phase ϕ [see Eq. (1)] which is measurable.

In the case of high x-ray frequency ($p \gg 1$) $\Delta_{at}(p, \theta) \sim -\sin \delta(t_0) \cos \theta (2 \cos^2 \theta - a_2)$ reflecting the $1s$ (via the factor $\cos \theta$) and $2p_0$ [via the factor $(2 \cos^2 \theta - a_2)$] interfering photoionization amplitudes.

Figure 2(a) shows the normalized momentum asymmetry of the initial coherent state ($1s+2p$) in the H atom obtained from (1) by integrating over the momentum at fixed polar angle $\theta=30^\circ$. It is compared to the photoelectron asymmetry given in Eq. (7) produced with $\tau_{FWHM}=100$ asec x-ray pulses with peak energies of $\Omega_x=50$ and 150 eV. Since the ionizing pulse duration is shorter than the oscillation period of the electron motion, the photoelectron spectra originated from two states overlap and interfere, as shown in the inset of Fig. 3. This interference is the origin of the observed asymmetry of the photoelectrons. Note that the two-level initial state can

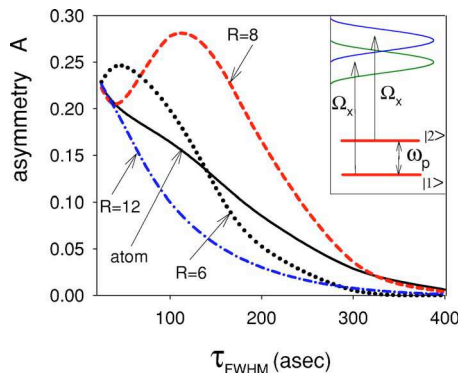


FIG. 3. (Color online) The atomic (solid line) and molecular (dashed line) asymmetries (7) as functions of pulse duration τ_{FWHM} . The phase shift, polar angle, and photon energy are $\delta=17$, $\theta=30^\circ$, and $\Omega_x=150$ eV.

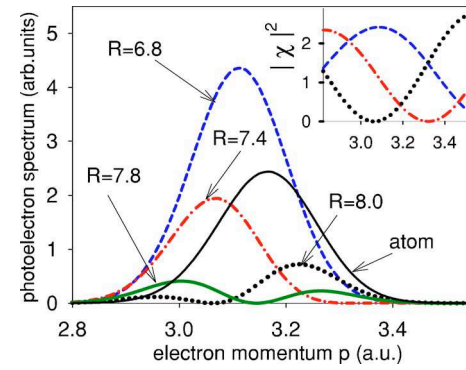


FIG. 4. (Color online) Atomic and molecular photoelectron spectra at the phase shift $\delta=17$ and different internuclear distances. The pulse duration, polar angle, and photon energy are $\tau_{FWHM}=100$ asec, $\theta=30^\circ$ and $\Omega_x=150$ eV.

be characterized by the dipole moment $d(t) = -2\alpha_1\alpha_2\langle 1|z|2\rangle\cos \delta(t)$. Zeros and extrema in the momentum asymmetry and in the time derivative of the dipole moment $\dot{d}(t) \sim \sin \delta(t)$ coincide.

We also see in Fig. 2(a) that the initial momentum asymmetry is projected into the continuum by attosecond photoionization. Slight phase deviation in the oscillation of photoelectron asymmetry is due to the Coulomb potential. In the remaining figures we illustrate results at the angle $\theta=30^\circ$ and x-ray photon energy 150 eV because it reproduces the initial momentum distribution better than at 50 eV.

In Fig. 2(b) we compare molecular ($\sigma_g 1s + \sigma_u 2p_0$) and atomic ($1s + 2p_0$) asymmetries. We show R and δ dependencies of the momentum asymmetry produced by attosecond photoionization. The most striking aspect of the figure is that the period and phase of the asymmetries depend only on δ . This is implicit in the Eq. (11) used for the calculation. However, δ is R dependent through ΔI_p for molecules. Another R dependence arises through the interference factor χ [Eq. (3)]. It is responsible for the R dependence of the amplitude of asymmetry. It can be shown that the positions of the maxima, minima, and zeros in the asymmetry do not depend on the attosecond pulse duration. If Fig. 2(b) was replotted for $\tau_{FWHM}=250$ asec, only the magnitude of the asymmetry (but not its sign) changes.

Figure 3 shows the normalized asymmetries for the atomic and molecular (for $R=6, 8,$ and 12 a.u.) cases as a function of the duration τ of the x-ray pulse. The R dependence of the molecular asymmetry arises from the interference of the two-center electron source influenced by the Coulomb potential. This interference modulates the asymmetry (Fig. 3), and spectrum (Fig. 4). As the pulse duration increases, the bandwidth of the photoelectrons emitted from each state decreases until there is no spectral overlap (see inset). Interference is no longer possible. In other words, as the pulse duration approaches $T=2\pi/\Delta I_p$, the period of the oscillations (Fig. 1), both the atomic and molecular momentum asymmetries disappear. An attosecond pulse can measure coherent electron oscillation or the oscillation can measure the duration of the attosecond pulse.

In Figs. 3 and 4 we chose the the time of the probe pulse

to be $\delta=17$, because the asymmetries near this point reach their maxima and the electron is maximally delocalized. This introduces an R -dependence molecular interference to the spectrum as seen in Fig. 4. Mathematically, the momentum distribution of the atom is modulated by a molecular contribution through the factor χ . The inset in Fig. 4 shows $|\chi|^2$ as a function of the electron momentum for different internuclear distances. The positions of the minima in Fig. 4 and its inset coincide. The maxima and minima arise from the photoelectron originating from the two-center potential and interfering in the Coulomb modified molecular continuum. The atomic and molecular oscillation periods corresponding to the spectra in Fig. 4 are $T_{at} \approx 405$ asec and $T_{mol} \approx 298$ asec at $R=6.8$ a.u.

In conclusion, attosecond pulses, because of their large energy bandwidth and high frequency, project bound-state

electron wave packets into the continuum. There, the wave packet can be fully characterized through its angle-resolved photoelectron spectrum. In practice, current attosecond laser sources are not intense enough and operate at a low repetition rate, making a full reconstruction impractical. However, they are perfectly adequate to resolve attosecond dynamics by measuring the changing momentum asymmetry of the spectrum. This would allow attosecond electron dynamics experiments that are analogous to vibrational dynamics experiments, which have been so influential in photochemistry [18]. As much higher repetition rate systems are developed [19] full characterization of both the spatial and temporal structures of electron wave packets will become possible.

We are grateful to F. Krausz and J.-C. Kieffer for valuable discussions.

-
- [1] M. Drescher *et al.*, Nature (London) **419**, 803 (2002).
 [2] A. Baltuška *et al.*, Nature (London) **421**, 611 (2003); R. Kienberger *et al.*, *ibid.* **427**, 817 (2004).
 [3] Y. Mairesse *et al.*, Science **302**, 1540 (2003).
 [4] P. Agostini and L. F. DiMauro, Rep. Prog. Phys. **67**, 813 (2004).
 [5] R. López-Martens *et al.*, Phys. Rev. Lett. **94**, 033001 (2005).
 [6] J. Itatani *et al.*, Laser Phys. **14**, 344 (2004).
 [7] Y. Mairesse and F. Quéré, Phys. Rev. A **71**, 011401(R) (2005); F. Quéré, Y. Mairesse, and J. Itatani, J. Mod. Opt. **52**, 339 (2005).
 [8] E. Cormier *et al.*, Phys. Rev. Lett. **94**, 033905 (2005).
 [9] A. D. Bandrauk, S. Chelkowski, and N. H. Shon, Phys. Rev. A **68**, 041802 (2003); A. B. H. Yedder *et al.*, *ibid.* **69**, 041802(R) (2004).
 [10] S. Chelkowski, A. D. Bandrauk, and A. Apolonski, Phys. Rev. A **70**, 013815 (2004).
 [11] E. Goulielmakis *et al.*, Science **305**, 1267 (2004).
 [12] H. Niikura, D. M. Villeneuve, and P. B. Corkum, Phys. Rev. Lett. **94**, 083003 (2005); H. Niikura *et al.*, J. Mod. Opt. **52**, 453 (2005).
 [13] A. D. Bandrauk, S. Chelkowski, and H. S. Nguyen, Int. J. Quantum Chem. **100**, 834 (2004).
 [14] H. Niikura *et al.*, Nature (London) **417**, 917 (2002); **421**, 826 (2003).
 [15] J. Ullrich *et al.*, Rep. Prog. Phys. **66**, 1463 (2003); C. Dimopoulou *et al.*, J. Phys. B **38**, 593 (2005).
 [16] T. Weber *et al.*, Phys. Rev. Lett. **92**, 163001 (2004); Nature (London) **431**, 437 (2004); A. L. Landers *et al.*, Phys. Rev. A **70**, 042702 (2004).
 [17] B. Joulakian *et al.*, Phys. Rev. A **54**, 1473 (1996).
 [18] A. H. Zewail, J. Phys. Chem. A **104**, 5660 (2000).
 [19] R. J. Jones *et al.*, Phys. Rev. Lett. **94**, 193201 (2005).